

Gluon saturation and inclusive hadron production at LHC

Eugene Levin^{1,2} and Amir H. Rezaeian¹

¹ *Departamento de Física, Universidad Técnica Federico Santa María,
Avda. España 1680, Casilla 110-V, Valparaíso, Chile*

² *Department of Particle Physics, Tel Aviv University, Tel Aviv 69978, Israel*
(Dated: May 31, 2019)

In high density QCD the hadron production stems from decay of mini-jets that have the transverse momenta of the order of the saturation scale. It is shown in this paper that this idea is able to describe in a unique fashion both the inclusive hadron production for $\sqrt{s} \geq 546$ GeV including the first data from LHC and the deep inelastic scattering at HERA. Recently reported data from ALICE, CMS and ATLAS including inclusive charged-hadron transverse-momentum and multiplicity distribution in pp collisions are well described in our approach. We provide predictions for the upcoming LHC measurements.

I. INTRODUCTION

The first LHC data [1–4] on inclusive hadron production call for a theoretical understanding of these processes based on QCD. At first sight the inclusive hadron production is a typical process that occurs at long distances where one has to use the non-perturbative methods of QCD. Therefore, the field of long distance processes seems to be a relevant subject to the domain of high-energy phenomenology with the main ingredients: soft Pomeron and secondary Reggeons. Such phenomenology is able to describe inclusive hadron production data (see Ref. [5] and references therein) but cannot be considered satisfactory since both soft Pomerons and Reggeons cannot be explained in terms of QCD ingredients; quarks and gluons. It should be also mentioned that the increase with energy of the average transverse momentum of the produced hadron observed experimentally [2, 3] cannot be explained in the Reggeon approach.

However, high density QCD [6–12] leads to a completely different picture of inclusive hadron production. In this approach the system of parton (gluons) at high energy forms a new state of matter: Color Glass Condensate (CGC). In the CGC picture, at high energy the density of partons ρ_p with the typical transverse momenta less than Q_s reaches a high value, $\rho_p \propto 1/\alpha_s \gg 1$ (α_s is the strong coupling constant). Q_s is the new momentum scale (saturation momentum) that increases with energy. At high energies/small Bjorken- x , $Q_s \gg \mu$ where μ is the scale of soft interaction. Therefore, $\alpha_s(Q_s) \ll 1$ and this fact allows us to treat this system on solid theoretical basis. On the other hand, even though the strong coupling α_s becomes small due to the high density of partons, saturation effects, the fields interact strongly because of the classical coherence. This leads to the a new regime of QCD with non-linear features which cannot be investigated in a more traditional perturbative approach.

In the framework of the CGC approach the secondary hadrons are originated from the decay of gluon mini-jets with the transverse momentum equal to the saturation scale $Q_s(x)$. The first stage of this process is under full theoretical control and determines the main characteristics of the hadron production, especially as far as energy, rapidity and transverse momentum dependence are concerned. The jet decay, unfortunately, could be treated mostly phenomenologically. However, we can hope that the phenomenological uncertainties would be reduced to several constants whose values will be extracted from the experiment.

Actually, such a description has passed the first check with the experimental data: the KLN paper [13] explains the main features of inclusive hadron production in heavy ion-ion and hadron-ion as well as proton-proton collisions [14] at RHIC. In this paper we wish to improve the KLN approach by introducing two new elements: the probability to find gluon with fixed transverse momentum that describes the deep inelastic scattering (DIS) data and that satisfies the Balitsky-Kovchegov [9, 11] non-linear equation; and a different description of inclusive hadron production at low transverse momenta of gluons. Over all success of our description indicates universality of the saturation physics which can be further tested at LHC and future collider experiment.

In the next section we discuss the k_t -factorization and main formulas that we use. In particular, we consider the interrelation between the color dipole scattering amplitude and the unintegrated gluon density that follows from the recent development of high density QCD [15]. An important improvement here to the previous works based on the KLN approach is the explicit inclusion of the impact-parameter dependence of the saturation scale. Section III is devoted to comparison with the experimental data and to discussion of various predictions for higher LHC energies. As a conclusion, in Sec. IV we highlight our main results and predictions for LHC.

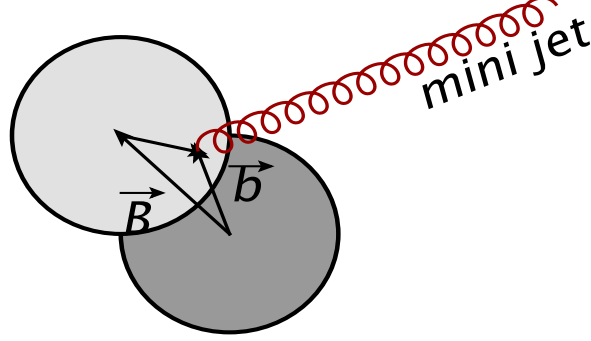


FIG. 1: Mini-jet production in hadron-hadron collisions in the transverse plane. The impact-parameter between two hadrons is \vec{B} .

II. INCLUSIVE GLUON PRODUCTION IN HIGH DENSITY QCD

The gluon jet production in hadron-hadron collisions can be described by k_t -factorization given by [15],

$$\frac{d\sigma}{dy d^2p_T} = \frac{2\alpha_s}{C_F} \frac{1}{p_T^2} \int d^2\vec{k}_T \phi_G^{h_1}(x_1; \vec{k}_T) \phi_G^{h_2}(x_2; \vec{p}_T - \vec{k}_T), \quad (1)$$

where $x_{1,2} = (p_T/\sqrt{s})e^{\pm y}$, and p_T and y is the transverse momentum and rapidity of the produced gluon jet. $\phi_G^{h_i}$ are the probability to find a gluon that carries x_i fraction of energy with k_T transverse momentum and $C_F = (N_c^2 - 1)/2N_c$ is the $SU(N_c)$ Casimir operator in the fundamental representation with the number of colors equals N_c .

For a proof of k_t -factorization see Ref. [15] and also Refs. [16–20] which confirm the former proof¹. However, we need to recall that the proof for the k_t -factorization was given for the scattering of a diluted system of partons, say for virtual photon, with a dense one. Our main idea is that we have gluon saturation for proton-proton scattering or in other words, we are dealing with interactions of two dense systems of partons (gluons). Therefore, the k_t -factorization has to be considered here as an assumption. Nevertheless, we believe that the k_T -factorization is currently the best tools at our disposal for the processes considered in this paper.

The unintegrated gluon density $\phi_G^{h_i}(x_i; \vec{k}_T)$ and color dipole-proton forward scattering amplitude $N(x_i, r_T; b)$ are related in a very specific way [15]. This relation reads as follows

$$\phi_G^{h_i}(x_i; \vec{k}_T) = \frac{1}{\alpha_s} \frac{C_F}{(2\pi)^3} \int d^2\vec{b} d^2\vec{r}_T e^{i\vec{k}_T \cdot \vec{r}_T} \nabla_T^2 N_G^{h_i}(y_i = \ln(1/x_i); r_T; b), \quad (2)$$

with

$$N_G^{h_i}(y_i = \ln(1/x_i); r_T; b) = 2N(y_i = \ln(1/x_i); r_T; b) - N^2(y_i = \ln(1/x_i); r_T; b), \quad (3)$$

where $N(y_i = \ln(1/x_i); r_T; b)$ is the dipole-hadron (h_i) forward scattering amplitude which satisfies the Balitsky-Kovchegov equation. In the above, r_T denotes the transverse dipole size and \vec{b} is the impact parameter of the scattering.

Eq. (3) looks very natural at large N_c . Indeed, for the color dipole amplitude in the Glauber form $N = 1 - \exp(-\Omega/2)$ (Ω is the opacity), equation Eq. (3) leads to $N_G = 1 - \exp(-\Omega)$ as it should be for the scattering of the two dipoles of the same sizes. We recall that a colorless gluon-probe just creates such two quark-antiquark dipoles, and the N_G is directly related to the gluon density.

Substituting Eq. (2) in Eq. (1), and after analytically performing some integrals, we obtain [15]

$$\frac{d\sigma}{dy d^2p_T} = \frac{2C_F}{\alpha_s(2\pi)^4} \frac{1}{p_T^2} \int d^2\vec{b} d^2\vec{B} d^2\vec{r}_T e^{i\vec{k}_T \cdot \vec{r}_T} \nabla_T^2 N_G^{h_1}(y_1 = \ln(1/x_1); r_T; b) \nabla_T^2 N_G^{h_2}(y_2 = \ln(1/x_2); r_T; |\vec{b} - \vec{B}|). \quad (4)$$

¹ Ref. [21] states that Eq. (1) is not correct. Unfortunately, there is no discussions in the paper why their result is so different from the other published papers. However, we have recently learned (Kovchegov, private communication) that M. A. Braun is successfully working on a proof showing that Ref. [21] actually leads to the k_t -factorization.

In the above equation, \vec{B} is the impact parameter between center of two hadrons and \vec{b} is the impact parameter of the produced mini-jet from the center of the hadron, see Fig. 1.

A. Choice of color dipole scattering amplitude

As it can be seen from Eq (2,4), we need here an impact-parameter dependent color-dipole forward amplitude. We will show later that the inclusion of the impact-parameter is very important in our approach and should not be ignored. The dipole-proton forward scattering amplitude $N(r, b; Y)$ can be in principle found by solving the perturbative nonlinear small-x Balitsky-Kovchegov (BK) [9, 11] or Jalilian-Marian-Iancu-McLerran-Weigert-Leonidov-Kovner (JIMWLK) [12] quantum evolution equations. Unfortunately, numerical solution to these non-linear equations in the presence of the impact-parameter is very challenging [22] and is not yet available. Moreover, a numerical solution does not give us the full control on the phenomenological parameters that have been used and we certainly lose the transparency and simplicity of physical interpretation if we rely only on the numerical solutions. Therefore, we choose a different approach to the solution of the BK equation that was suggested in Ref. [23]. First, we recall that the BK equation predicts the geometric scaling behavior [24], namely the amplitude $N(r, b; Y)$ is not a function of three variables but it is a function of only one variable $z^2 = r^2 Q_s^2(x; b)$ ($N(r, b; Y) = F(z)$) where $Q_s(x; b)$ is the saturation momentum. We also know [25] the behavior of the scattering amplitude deeply in the saturation region ($z \gg 1$)

$$N(Y; r; b) = 1 - \exp\left(-\frac{\chi(\gamma_{cr})}{2(1-\gamma_{cr})} \ln^2 z\right), \quad (5)$$

where $\chi(\gamma)$ is the BFKL kernel

$$\omega(\gamma) = \bar{\alpha}_s \chi(\gamma) = \bar{\alpha}_s \{2\psi(1) - \psi(\gamma) - \psi(1-\gamma)\}, \quad (6)$$

with a notation $\bar{\alpha}_s = \alpha_s N_c / \pi$. In above, we define $\psi(x) = d \ln \Gamma(x) / dx$ and $\Gamma(x)$ is the Euler function. The parameter γ_{cr} is the solution to the following equation

$$\frac{d\chi(\gamma_{cr})}{d\gamma_{cr}} = -\frac{\chi(\gamma_{cr})}{1-\gamma_{cr}}. \quad (7)$$

In Ref. [25] a solution was found for the entire kinematic region for a simplified BFKL kernel, namely, instead of Eq. (6), the following kernel was used,

$$\omega(\gamma) = \bar{\alpha}_s \begin{cases} \frac{1}{\gamma} & \text{for } z = rQ_s \leq 1; \\ \frac{1}{1-\gamma} & \text{for } z = rQ_s > 1; \end{cases} \quad (8)$$

which describes only leading twist contribution to the full BFKL kernel of Eq. (6). The lesson from this solution is very instructive: for $r^2 Q_s^2 \leq 1$, the amplitude N satisfies the DGLAP (BFKL) linear evolution equation with the boundary condition $N(r, b; Y) = N_0 = \text{Constant}$ for $r^2 = 1/Q_s^2$ while for $r^2 Q_s^2 > 1$ we have solution that has the form of Eq. (5). Using these general features of the solution we choose the model suggested in Ref. [26] which improves the earlier studies on this line [23, 27]. In this model the color dipole-proton forward scattering amplitude is given by

$$N(Y; r; b) = \begin{cases} N_0 \left(\frac{z}{2}\right)^{2(\gamma_s + \frac{1}{\kappa \lambda Y} \ln(\frac{2}{z}))} & \text{for } z = rQ_s \leq 2; \\ 1 - \exp(-A \ln^2(Bz)) & \text{for } z = rQ_s > 2; \end{cases} \quad (9)$$

where the saturation scale Q_s is given by

$$Q_s = \left(\frac{x_0}{x}\right)^{\frac{\lambda}{2}} \exp\left\{-\frac{b^2}{4(1-\gamma_{cr})B_{CGC}}\right\}. \quad (10)$$

As we have already mentioned Eq. (9) as well as Eq. (10) has the form of the solution to the BK equation at a fixed QCD coupling. For $z < 1$ the effective anomalous dimension $\gamma_s + \frac{1}{\kappa \lambda Y} \ln(\frac{2}{z})$ with $\gamma_s = 1 - \gamma_{cr}$ follows from the BFKL (and DGLAP) equation in the vicinity of the saturation line (see Ref. [23] for the detailed derivation).

For the leading order BFKL kernel with frozen QCD coupling the parameters of Eq. (9) and Eq. (10) have the following values

$$1 - \gamma_{cr} = 0.63; \quad \lambda = \bar{\alpha}_s \frac{\chi(\gamma_{cr})}{1 - \gamma_{cr}} = 4.88\bar{\alpha}_s; \quad \kappa = \frac{\chi''(\gamma_{cr})}{\chi'(\gamma_{cr})} = 9.9. \quad (11)$$

The parameters A and B can be found from matching of N and its logarithmic derivatives at $z = 2$ while N_0 and B_{CGC} remain fitting parameters.

The advantage of Eq. (9) is that one has the possibility to take into account the next-to-leading order (NLO) corrections. It has been shown that the NLO correction to the BFKL equation (and therefore BK equation) are large and it changes considerably the value of λ from $\lambda \approx 0.9$ to $\lambda \approx 0.3$ for $\bar{\alpha}_s = 0.2$ [28, 29]. The value of γ_s in Eq. (9) is also affected by the NLO corrections as well as by the running QCD coupling [28–30]. It is therefore generally believed that the higher order corrections to the NLO BK equation should be important. In our phenomenological approach, we take the value of parameters λ, γ_s, N_0 and B_{CGC} obtained from a fit to the DIS data at HERA at small Bjorken- x $x < 0.01$ [26]. In order to simulate the behavior of gluon density at large $x \rightarrow 1$, we product the unintegrated gluon density with $(1 - x)^4$ as prescribed by quark counting rules [31].

B. Physical observables

The rapidity distributions of the min-jets can be calculated using Eq. (1),

$$\frac{dN_{\text{mini-jet}}}{d\eta} = h[\eta] \frac{1}{\sigma_{nsd}} \int d^2 p_T \frac{d\sigma}{dy d^2 p_T} [Eq. (1)], \quad (12)$$

where η is the pseudorapidity and $h[\eta]$ is the jacobian which takes account of the difference between rapidity y and the measured pseudo-rapidity η [13],

$$h(\eta, p_T) = \frac{\cosh \eta}{\sqrt{\frac{m_{jet}^2 + p_T^2}{p_T^2} + \sinh^2 \eta}}, \quad (13)$$

where m_{jet} is the mass of mini-jet. One also has to express rapidity y in Eq. (1) in terms of pseudo-rapidity η . This relation is given by

$$y(\eta, p_T) = \frac{1}{2} \ln \left\{ \frac{\sqrt{\frac{m_{jet}^2 + p_T^2}{p_T^2} + \sinh^2 \eta} + \sinh \eta}{\sqrt{\frac{m_{jet}^2 + p_T^2}{p_T^2} + \sinh^2 \eta} - \sinh \eta} \right\}. \quad (14)$$

The mass of the mini-jet is approximately equal to $m_{jet}^2 \simeq 2\mu p_T$ (see Ref. [13]) where μ is the scale of soft interaction. One can see that Eq. (1) has the infrared divergence at $p_T \rightarrow 0$ for the kinematic region $k_T \gg p_T$. In Ref. [13] it was suggested to integrate over $k_T \leq p_T$. The reason is that such an integration reproduces the factorization formula at large $p_T \gg \mu$ for the DGLAP evolution. We think that it is more natural in our approach to replace p_T by $\sqrt{p_T^2 + m_{jet}^2}$ everywhere in Eq. (1), namely in the evaluation of x_1, x_2 and also in the denominator $1/p_T^2$.

In Eq. (12) we do not take into account the fragmentation of the produced gluon (mini-jet) into hadrons. We rely on the principle of Local Parton-Hadron Duality (LPHD) [32, 33] namely the form of the rapidity distribution will not be distorted by the jet decay and only a numerical factor will differ the mini-jet spectrum from the hadron one. We believe that it is better to use the LPHD scheme than to deal with the fragmentation's functions for which we have no theoretical justifications at low p_T . It should be stressed that the same idea has been used in the KLN approach which describes the rapidity distribution of heavy-ion collisions data in a wide range of energies. This idea has also worked perfectly in e^+e^- annihilation into hadrons [32, 33].

We should stress that the value of inelastic non-singlet diffractive (NSD) cross-section σ_{nsd} cannot be calculated in our approach and has to be taken from the soft interaction models such as in Refs. [34, 35]. The NSD cross-section σ_{nsd} is defined as $\sigma_{nsd} = \sigma_{tot} - \sigma_{el} - \sigma_{sd} - \sigma_{dd}$ where σ_{el} , σ_{sd} and σ_{dd} are the cross sections of elastic, single and double diffraction, respectively. However, the experimental data on σ_{dd} is very limited [36], σ_{sd} is measured with rather large errors [37, 38] and even for the total cross-section σ_{tot} [38] we have two values at the Tevatron energies [39]. Therefore,

we should stress that in this way we can only predict $d\sigma/dy$ rather than dN_{ch}/dy . In order to overcome this problem, here we choose a different strategy: the physical meaning of σ_{nsd} in Eq. (12) is the area of interaction which can be calculated in our approach. Indeed, using Eq. (4) one can calculate the average impact parameter for the inclusive production of the mini-jet

$$\langle \vec{b}_{jet}^2 \rangle = \frac{\int \frac{d^2 p_T}{p_T^2} \int d^2 \vec{b} d^2 \vec{B} d^2 r_T \left(b^2 + |\vec{b} - \vec{B}|^2 \right) e^{i\vec{k}_T \cdot \vec{r}_T} \nabla_T^2 N_G^{h_1}(y_1 = \ln(1/x_1); r_T; b) \nabla_T^2 N_G^{h_2}(y_2 = \ln(1/x_2); r_T; |\vec{b} - \vec{B}|)}{\int \frac{d^2 p_T}{p_T^2} \int d^2 \vec{b} d^2 \vec{B} d^2 r_T e^{i\vec{k}_T \cdot \vec{r}_T} \nabla_T^2 N_G^{h_1}(y_1 = \ln(1/x_1); r_T; b) \nabla_T^2 N_G^{h_2}(y_2 = \ln(1/x_2); r_T; |\vec{b} - \vec{B}|)} \quad (15)$$

The NSD cross-section σ_{nsd} is then equal to the average interaction area upto a constant $\sigma_{NSD} = M\pi \langle \vec{b}_{jet}^2 \rangle$. The pre-factor M will be determined and discussed later.

The average transverse momentum of the mini-jet is defined in the usual way:

$$\langle p_{jet,T} \rangle = \int d\eta h[\eta] \int d^2 p_T |p_T| \frac{d\sigma}{d\eta d^2 p_T} [Eq. (1)] / \int d\eta h[\eta] \int d^2 p_T \frac{d\sigma}{d\eta d^2 p_T} [Eq. (1)]. \quad (16)$$

The advantage of this quantity is that it can be calculated without usual uncertainties associated with the soft interaction physics. The average transverse momentum of the jet can be directly related to the saturation scale via Eqs. (1,9,16) and it has the following simple form at large $Q_s \gg m_{jet}$,

$$\langle p_{jet,T} \rangle \propto \frac{Q_s}{\ln(Q_s^2/m_{jet}^2 + 1) + \mathcal{Q}}, \quad (17)$$

where the parameter \mathcal{Q} is of order of one and takes into account the contribution of integrals in Eq. (16) for $p_T > Q_s$.

In order to calculate the transverse momentum of hadrons which is measured experimentally, we need to recall that $\vec{p}_{hadron,T} = z\vec{p}_{jet,T} + \vec{p}_{intrinsic,T}$ which leads to

$$\langle p_{hadron,T} \rangle = \sqrt{\langle zp_{jet,T} \rangle^2 + \langle p_{intrinsic,T} \rangle^2}, \quad (18)$$

where z is the fraction of energy of the jet carried by the hadron. $\langle p_{intrinsic,T} \rangle$ is the average intrinsic transverse momentum of the hadron in the mini-jet. In other words, this is the transverse momentum of the hadron in the mini-jet that has only longitudinal momentum.

In the framework of the LHPD, the p_T spectrum of the produced hadron is equal to

$$\frac{dN_{hadron}}{d^2 p_T} = \int d\eta h[\eta] \frac{1}{\sigma_{nsd}} \frac{d\sigma}{d\eta d^2 p_{jet,T}} \left[Eq. (1) \text{ with } p_{jet,T} = p_T/z \right], \quad (19)$$

where in the above p_T is the transverse momentum of the produced hadron.

In the CGC scenario, the gluon saturation scale is proportional to the density of partons (see Refs. [13, 14]). The parton density is proportional to the multiplicity and, therefore, we can use the following expression for the saturation momentum in the event with the multiplicity of the hadrons n :

$$Q_s(n; x) = \frac{n}{\langle n \rangle} Q_s(x), \quad (20)$$

where $\langle n \rangle$ is the average multiplicity that has been measured in inclusive production without any selection related to multiplicity. Using Eq. (17) again one can relate the saturation scale at a given multiplicity to the average transverse momentum of the produced mini-jets at large $Q_s \gg m_{jet}$,

$$\langle p_{jet,T} \rangle \propto \frac{Q_s(n; x)}{\ln(Q_s^2(n; x)/m_{jet}^2 + 1) + \mathcal{Q}}. \quad (21)$$

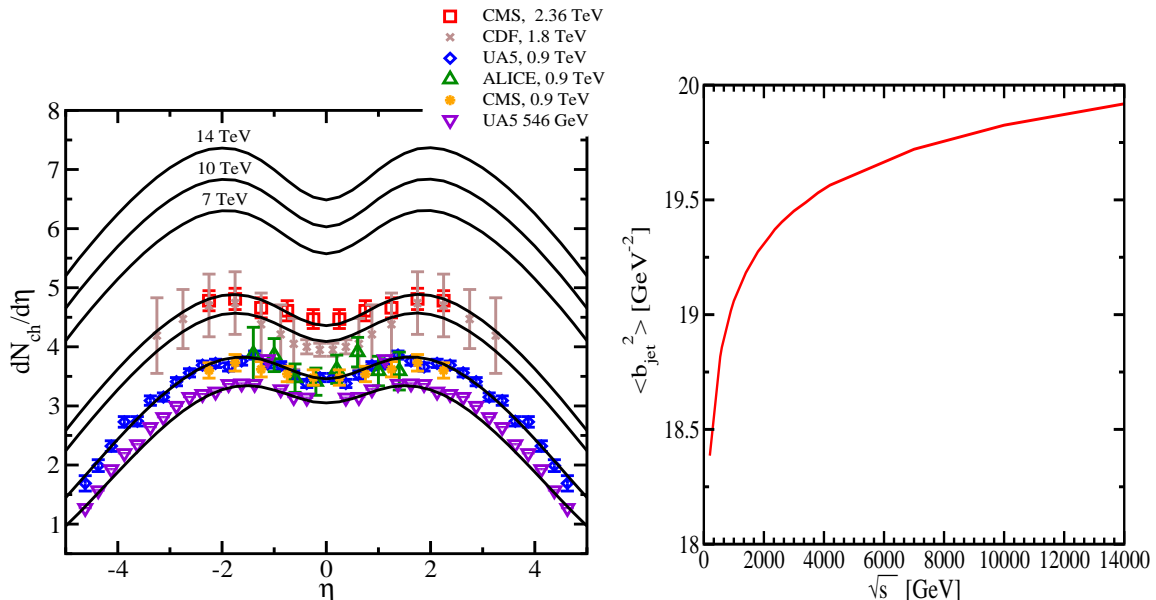


FIG. 2: Right: shows the average impact parameter of the produced mini-jet $\langle b_{jet}^2 \rangle$ given by Eq. (15) as function of energy. Left: The comparison with the experimental data and prediction for $dN_{ch}/d\eta$ using Eq. (12) with $\sigma_{nsd} = M\pi\langle b_{jet}^2 \rangle$. The curves are normalized by data at $\sqrt{s} = 546$ GeV, see the text for the details. The experimental data are from Refs. [1, 2, 41]. The error bars on the UA5 and ALICE data points are statistical. We show only systematic errors for the CMS data points.

III. COMPARISON WITH THE EXPERIMENTAL DATA AND PREDICTION FOR HIGHER ENERGIES

In the derivation of the k_t -factorization it was assumed that the strong coupling α_s is a constant. As a generalization, in Eq. (1) we replace α_s by $\alpha_s(p_T)$, where p_T is the transverse momentum of the mini-jet and in Eq. (2) we also replace $1/\alpha_s$ by $1/\alpha_s(Q_s(x_i))$ where $Q_s(x_i)$ is the saturation scale in hadron h_i . This seems to be the most natural way of introducing the running coupling which still preserves the form of Eq. (4) apart from the over-all factor outside of integrals which now depends on kinematics. Indeed the inclusion of running strong-coupling leads to improvement of our description. For the running strong coupling α_s , we employ the same scheme as used by the KLN approach [13], namely we use the leading-order running coupling with smooth freezing below the virtuality $Q^2 \approx 0.8 \text{ GeV}^2$ at the value of $\alpha_s^{IR} \approx 0.5$. This is in accordance with many evidence from jet physics which indicates that the QCD coupling may stay reasonably small, $\alpha_s^{IR} = 0.4 \div 0.6$ in the infrared region [40].

The impact-parameter dependence in our formulation emerges from the employed impact-parameter dependent saturation scale, see Eqs. (9,10). In this model, the profile of the saturation scale in the proton assumed to be a Gaussian. It is difficult to interpret the parameter B_{CGC} in Eq. (10) in terms of proton size due to the dipole size r and rapidity Y dependence of the anomalous dimension. Nevertheless, in order to have a intuitive picture, one may take $2B_{CGC}$ as relative average squared transverse radius of the proton. The value of $B_{CGC} = 7.5 \text{ GeV}^{-2}$ was obtained as a fit in order to describe the slope of t -distribution of diffractive processes at HERA [26], which in turn fix the normalization of the color dipole-proton cross-section. In Fig. 2 (right), we show the average impact parameter of jet $\langle \vec{b}_{jet}^2 \rangle$ from center of the hadrons. Notice that for obtaining $\langle \vec{b}_{jet}^2 \rangle$, the over-all coefficient in Eq. (15) will be dropped out and we are left with no free parameter. The $\langle \vec{b}_{jet}^2 \rangle$ is about $2.5B_{CGC}$ and it slightly increases with energy.

The mass of mini-jet m_{jet} is proportional to the saturation scale $m_{jet}^2 \simeq 2\mu p_T$ [13] since the typical transverse momentum of the mini-jets is the saturation scale Q_s and μ is the scale of soft interaction. The saturation scale in the CGC-b model Eq. (9) changes slowly with energy. For our interested range of energy considered in this paper at midrapidity $\eta = 0$ and $p_T = 1 \text{ GeV}$ for the central collisions $b = 0$, we have $Q_s \approx 0.6 \div 0.8 \text{ GeV}$. Taking the scale of soft interaction equal to pion mass $\mu \approx m_\pi = 0.14 \text{ GeV}$, we have $m_{jet} \approx 0.4 \div 0.5 \text{ GeV}$. We will first assume a fixed value for the mini-jet mass $m_{jet} = 0.4 \text{ GeV}$. To estimate the effect of the mini-jet mass, we will later consider a case with a different value for m_{jet} .

In order to obtain the multiplicity distribution of hadrons in pp collisions from the corresponding mini-jets pro-

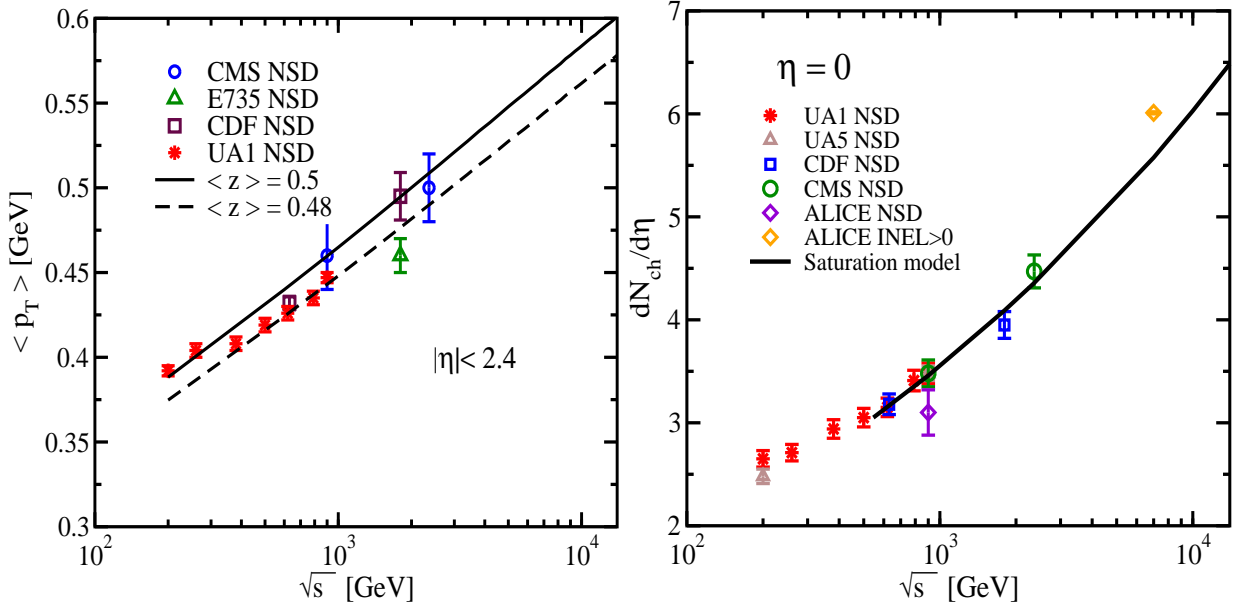


FIG. 3: Right: Energy dependence of the charged hadrons multiplicity in the central region of rapidity $\eta = 0$ in pp collisions. The theoretical curve is our prediction coming from the saturation model for the NSD interactions. Left: Energy dependence of the average transverse momentum of charged hadrons. The CMS data [2] points and the theoretical curves in the left panel are for $|\eta| < 2.4$. The experimental data are from Refs. [2, 4, 41–45]. The experimental error bars indicate systematic uncertainties.

duction cross-section Eqs. (1,12) we have to fix some unknown parameters. First, based on the gluon-hadron duality, the rapidity distribution of hadron and radiated mini-jets can be different by a factor C . Second, although the k_t -factorization incorporates the small- x evolution taking into account the higher-order gluon scatterings and non-linear gluon recombination effects, nevertheless given that we resort to a phenomenological color-dipole model, there might be still some extra contributions which are missed in our formulation. The discrepancy between the exact calculation and our formulation can be then effectively taken into account with a extra K -factor. Finally, in order to obtain the charged-particle multiplicity, we should divide the mini-jet cross-section with non-singlet diffractive cross-section which as we already discussed is obtained via $\sigma_{nsd} = M\pi \langle \tilde{b}_{jet}^2 \rangle$ with a new unknown dimensionless parameter M . Fortunately, these three unknown pre-factors C , K and M appear as a product and can be reduced to only one unknown parameter which will be determined with a fit to the experimental data for the charged particle multiplicity $\frac{dN_{ch}}{d\eta}$ at midrapidity for the lowest energy considered here $\sqrt{s} = 546$ GeV. Therefore, we obtain $\frac{KC}{M} = 2.32$ at $\sqrt{s} = 546$ GeV. We assume that this over-all normalization factor is energy-independent. Then for higher energy $\sqrt{s} > 546$ GeV, we do not have any free parameters in our calculation and our results may be considered as predictions of the model. Notice that we have employed a color-dipole model that its free parameters was obtained from a fit to the HERA data for $x_B < 0.01$ and $Q^2 \in [0.25, 45]$, therefore our formulation is less reliable at lower energies (now used here). In Fig. 2 (left), we show the charged multiplicity distribution for pp collisions at various energies. Our model gives a good description of all available data for $\sqrt{s} \geq 546$ GeV including the recently released data from ALICE [1], CMS [2] and ATLAS [3] at 0.9 and 2.36 TeV. We also show our predictions for the LHC energies at 7, 10 and 14 TeV. It is seen that as the energy increases the peak of rapidity distribution at forward (backward) becomes more pronounced. This effect has been also observed in Ref. [46] where it was shown that the rapidity dependence of the invariant cross-section for both identified hadrons and direct photon has a peak at forward rapidities and this peak will be further enhanced by saturation effects [46].

In Fig. 3 (right) we show the charged-hadron pseudorapidity density in the central region $\eta = 0$ as a function of center-of-mass energy in pp collisions. Notice that since our prescription is valid only for the NSD interactions we do not show the corresponding data for the inelastic event selection. We have also shown recently reported charged-particle pseudorapidity density from ALICE [4] at 7 TeV in $|\eta| < 1$ for inelastic collisions with at least one charged particle in that region (denoted by INEL > 0). Again this point is out of the scope of our calculation and we did not expect to explain it. Notice that we expect less than 20 – 30% error in our calculation at higher energy due to the uncertainty associated with our choice of a fixed mini-jet mass of 0.4 GeV for all energies.

The average transverse momentum of charge hadrons can be obtained from Eq. (18). In Eq. (18), the average intrinsic transverse momentum of hadron has a purely non-perturbative origin and is due to the finite-size effect of

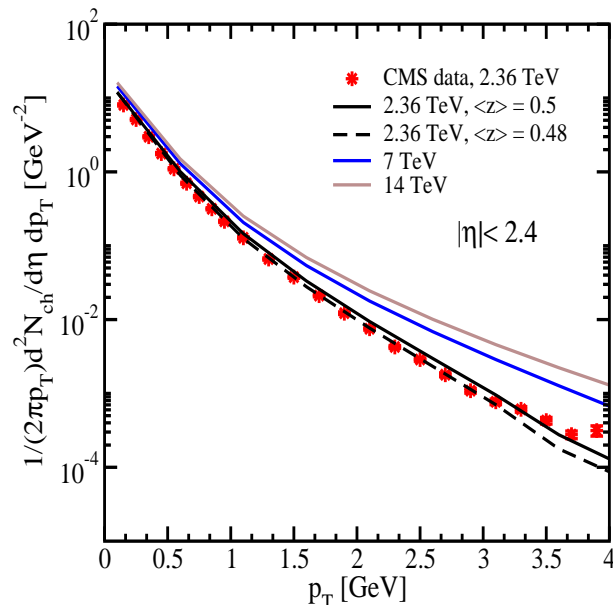


FIG. 4: The differential yield of charged hadrons for $|\eta| < 2.4$. The experimental data are from CMS [2] at 2.36 TeV for $|\eta| < 2.4$. We show also our theoretical predictions for 7 and 14 TeV with $\langle z \rangle = 0.5$. The experimental error bars shown are systematic and statistical errors added linearly.

hadrons. We take $\langle p_{\text{intrinsic},T} \rangle$ equal to the pion mass, the scale of soft-interaction $\mu = m_\pi$ throughout this paper. In order to obtain the average transverse momentum of charge hadrons, we need also to know the value of the average momentum fraction of mini-jets carried by the hadrons $\langle z \rangle$. It is seen from Fig. 3 (left) that an average value of $\langle z \rangle = 0.48 \div 0.5$ is remarkably able to describe the average transverse momentum of charge hadrons in a wide range of energies. Our theoretical curves and CMS data [2] are for the range $|\eta| < 2.4$. One may also estimate the value of $\langle z \rangle$ from the fragmentation functions, having in mind that the $\langle z \rangle$ for mini-jets in parton-hadron duality picture is not necessarily the same as the corresponding average of fragmentation momentum of the produced gluons in the parton model. Nevertheless, employing recently developed AKK08 fragmentation functions [47] for charged hadrons production from a gluon, one obtains $\langle z \rangle = 0.5$ on average over low p_T within the range of $1 < p_T$ [GeV] ≤ 2 (AKK's fragmentation is valid only for $Q > 1$ GeV). In order to further test the validity of the value $\langle z \rangle \approx 0.5$ for the mini-jets, we show in Figs. 4, 5 (top panel) our predictions obtained from Eq. (19) for the differential yield of charged hadrons in the range $|\eta| < 2.4$ and at various $|\eta|$ bins for $\sqrt{s} = 2.36$ TeV. The experimental data are recently reported from CMS collaboration [2]. It is seen that our results is in quite good agreement with experimental data. We recall again that the pre-factor in Eq. (19) is the same as what we already fixed with experimental multiplicity data at low-energy $\sqrt{s} = 546$ GeV at $\eta = 0$. Therefore, we have no free parameters in obtaining the theoretical curves in Figs. 4, 5 (top). In Figs. 4, 5 (top), we have also shown our predictions for $\sqrt{s} = 7$ and 14 TeV. The fact that our model reasonably works at low p_T (for $\sqrt{s} = 2.36$ TeV) is due to the fact that the saturation scale is rather large at low p_T , for $p_T \approx m_\pi$ we have $Q_s \approx 1$ GeV in the central rapidity region.

In Fig. 5, it is seen a peculiar peak of the charged hadrons production rate at low $p_T \approx 0.2$ GeV. Actually the appearance of such a peak is expected in our formulation. Notice that from Eq. (12) the differential yield of charged hadrons has a form $\frac{d^2 N}{d\eta dp_T} \propto \frac{2\pi p_T}{p_T^2 + \langle z \rangle^2 m_{jet}^2} \mathcal{F}(x_1, x_2, p_T)$ where \mathcal{F} is an analytic function. At $p_T = 0$ trivially we have $\frac{d^2 N}{d\eta dp_T} = 0$, for $p_T < m_{jet} \langle z \rangle$ the spectra is a monotonically increasing function of p_T and for $p_T > m_{jet} \langle z \rangle$ it is decreasing due to the denominator. The position of the peak is then approximately at $p_T \simeq m_{jet} \langle z \rangle \approx 0.2$ GeV since we have $\langle z \rangle = 0.5$ and $m_{jet} = 0.4$ GeV. This simple picture is consistent with the CMS experimental data [2] shown in Fig. 5 (top).

In order to see more clearly the effect of the mini-jet mass m_{jet} , in Fig. 5 (down) we compare the differential yield of charged hadrons calculated with two different values for the mini-jet mass $m_{jet} = 0.4$ and 0.8 GeV. We also show the multiplicity distribution in the inserted panel in Fig. 5. As we already pointed out, the mass of mini-jet is controlled by the saturation scale. Obviously from the saturation scale in our model, $m_{jet} = 0.8$ GeV is too large. Therefore, it is not surprising that the description of experimental data for both multiplicity and spectra worsened for such a large mini-jet mass. Nevertheless, it is obvious from Fig. 5 that the position of the peak moves to a higher p_T for a larger mini-jet mass. Note that the CMS experimental data [2] at $\sqrt{s} = 2.36$ TeV for the average transverse momentum of

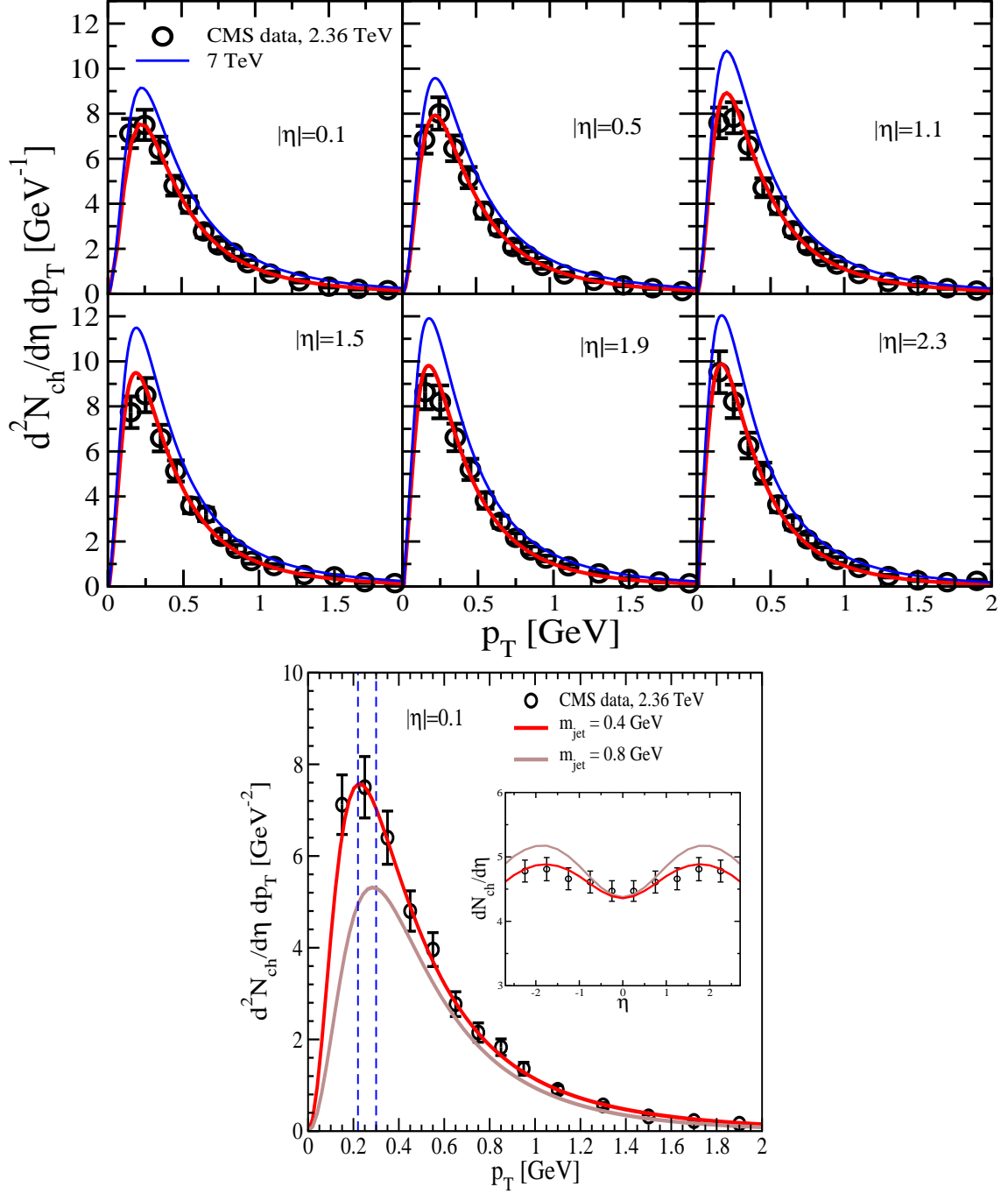


FIG. 5: Upper panel: The differential yield of charged hadrons in various $|\eta|$ bins for $\sqrt{s} = 2.36$ TeV. The experimental data are from CMS [2]. We also show our predictions for 7 TeV. The experimental errors shown are systematic and statistical errors added linearly. Lower panel: The differential yield of charged hadrons for $|\eta| = 0.1$ for two different value of mini-jet masses m_{jet} . The inserted plot in the lower panel figure shows the charged hadrons multiplicity again for two values of m_{jet} for the same energy.

charged hadrons can be reproduced with $\langle z \rangle = 0.37$ when $m_{jet} = 0.8$ GeV. Again the position of the peak in spectra is consistent with simple formula $p_T \simeq m_{jet} \langle z \rangle \approx 0.3$ in accordance with the full calculation shown in Fig. 5. Notice that in our model calculation shown in Fig. 5 (top), the position of the peak persists at various rapidities bin (and energies) since we have taken a fixed m_{jet} for simplification. To conclude, a precise measurement of the differential yield of charged hadrons at low p_T for higher energies at LHC will provide valuable information about the mini-jet mass and its connection with the gluon saturation.

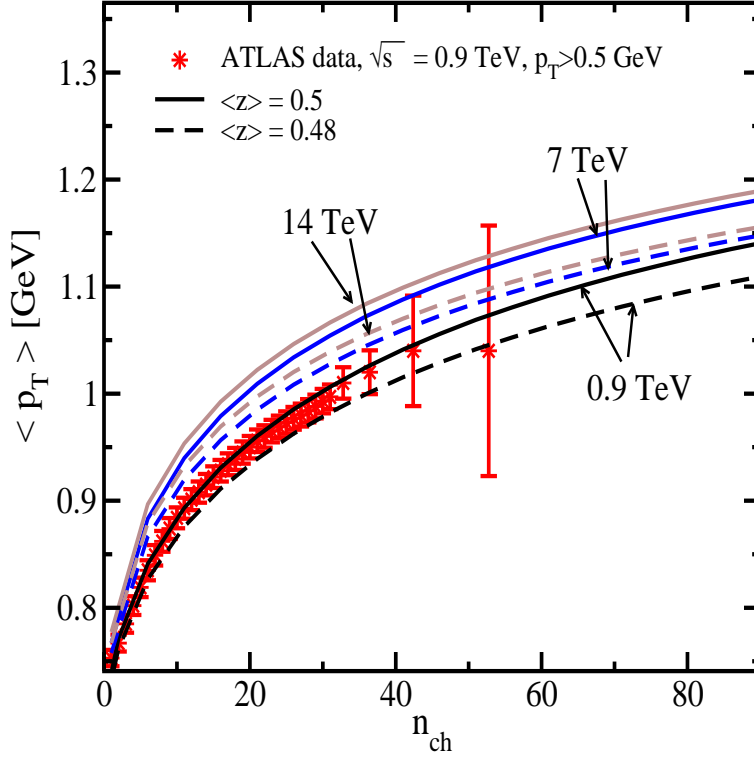


FIG. 6: The average transverse momentum of charged hadrons as a function of the number of charged particles for events with $n_{ch} \geq 1$ within the kinematic range $p_T > 500$ MeV. The experimental data are from ATLAS for $\sqrt{s} = 0.9$ TeV and $|\eta| < 2.5$ [3]. The theoretical curves were obtained for $|\eta| = 0$ and with the same kinematic constraint $p_T > 500$ MeV at various energies for two values of $\langle z \rangle = 0.48, 0.5$ corresponding to the dashed and the solid lines, respectively. We only show the systematic experimental errors.

In Fig. 6, we show the average transverse momentum of charged hadrons as a function of the number of charged particles for events within the kinematic range $p_T > 500$ MeV. The experimental data are from ATLAS for $\sqrt{s} = 0.9$ TeV [3]. The saturation scale at various multiplicity is given by Eq. (20) where $\langle n \rangle$ can be conceived as a normalization and its value is taken to be the charged multiplicity at midrapidity $\eta = 0$ for a given center-of-mass energy (shown in Fig. 4 (right)). In order to implement in our calculation the experimental kinematic constraint $p_T > 500$ MeV on the measured events, we impose that $\langle p_{\text{intrinsic},T} \rangle > 500$ MeV. To this end, we take $\langle p_{\text{intrinsic},T} \rangle = (m_\rho + m_k)/2$ where the mass of ρ and k mesons are $m_\rho = 775$ MeV and $m_k = 497$ MeV, respectively. In Fig. 6, we show $\langle p_T \rangle$ for two values of $\langle z \rangle$. It is seen that our model is able to give a very good description of the ATLAS data. We have also shown in the same plot, our predictions for the higher LHC energies.

The general behavior of the theoretical curves shown in Fig. 3 (left) and Fig. 6 for the average transverse momentum of the produced hadrons is in accordance with a simple formula given in Eqs. (17,21) showing a clear connection between the gluon saturation and the measured transverse momentum of charged hadrons.

IV. CONCLUSION

In high density QCD the main source of hadron production is the decay of gluon mini-jets with the transverse momentum of the order of the saturation scale. This viewpoint is based on the fact that the system of partons (gluons) creates a new state of matter, the so-called Color Glass Condensate, in which the gluon density reaches the limited values of the order of $1/\alpha_s$ with new typical transverse momentum (the saturation scale). We developed a model that includes the gluon saturation and demonstrated that this model is able to describe both the inclusive hadron production at high energies including the first data from the LHC and the deep inelastic scattering data from HERA in a unique fashion.

We predicted an increase of $dN_{ch}/dy|_{\eta=0}$, mean transverse momentum and the multiplicity of produced charged hadrons with energy which is in accordance with the first LHC data measured by ALICE [1, 4], CMS [2] and ATLAS [3] collaboration, see Figs. 2,3,6. In the framework of high density QCD all these phenomena are closely related to the

growth of the saturation momentum as a function of energy and of density of partons. It should be stressed that the other high-energy phenomenological approaches cannot describe the dependence of the average transverse momentum of the produced hadron on energy and hadron multiplicities.

We showed that recently reported data by the CMS collaboration [2] on the differential yield of charged hadrons at low p_T for $\sqrt{s} = 2.36$ TeV reveal an interesting information on the mini-jets production and its connection with the saturation. We showed that the appearance of a peak in differential yield of charged hadrons at low p_T is closely related to the mini-jet mass and the value of the saturation scale.

We provided various predictions for the upcoming LHC measurements at higher energies in pp collisions. We believe that this paper will be useful for the microscopic interpretation of the upcoming LHC data and will lead to a deeper understanding of the hadron interactions at high energy in the framework of QCD.

The particle production scheme presented in this paper can be also applied to the calculation of inclusive hadron production in heavy ion collisions at LHC. We are currently working on this problem and plan to report on this in the near future.

Acknowledgments

This work was supported in part by Conicyt Programa Bicentenario PSD-91-2006 and the Fondecyt (Chile) grants 1090312 and 1100648.

-
- [1] ALICE Collaboration, Eur. Phys. J. C **65** (2010) 111 [arXiv:0911.5430]; arXiv:1004.3034.
 - [2] CMS Collaboration, JHEP **1002** (2010) 041 [arXiv:1002.0621].
 - [3] ATLAS Collaboration, Phys. Lett. **B688** (2010) 21 [arXiv:1003.3124].
 - [4] ALICE Collaboration, arXiv:1004.3514.
 - [5] E. Gotsman, E. Levin and U. Maor, Phys. Rev. D **81** (2010) 051501 [arXiv:1001.5157].
 - [6] L. V. Gribov, E. M. Levin and M. G. Ryskin, Phys. Rep. **100** (1983) 1.
 - [7] A. H. Mueller and J. Qiu, Nucl. Phys. **B268** (1986) 427.
 - [8] L. McLerran and R. Venugopalan, Phys. Rev. **D49** (1994) 2233, 3352; **D50** (1994) 2225; **D53** (1996) 458; **D59** (1999) 09400.
 - [9] I. Balitsky, [arXiv:hep-ph/9509348]; Phys. Rev. **D60** (1999) 014020 [arXiv:hep-ph/9812311].
 - [10] A. H. Mueller, Nucl. Phys. **B415** (1994) 373; **B437** (1995) 107.
 - [11] Y. V. Kovchegov, Phys. Rev. **D60** (1999) 034008 [arXiv:hep-ph/9901281].
 - [12] J. Jalilian-Marian, A. Kovner, A. Leonidov and H. Weigert, Phys. Rev. **D59** (1999) 014014 [arXiv:hep-ph/9706377]; Nucl. Phys. **B504** (1997) 415 [arXiv:hep-ph/9701284]; J. Jalilian-Marian, A. Kovner and H. Weigert, Phys. Rev. **D59** (1999) 014015 [arXiv:hep-ph/9709432]; A. Kovner, J. G. Milhano and H. Weigert, Phys. Rev. **D62** (2000) 114005 [arXiv:hep-ph/0004014]; E. Iancu, A. Leonidov and L. D. McLerran, Phys. Lett. **B510** (2001) 133 [arXiv:hep-ph/0102009]; Nucl. Phys. **A692** (2001) 583 [arXiv:hep-ph/0011241]; E. Ferreira, E. Iancu, A. Leonidov and L. McLerran, Nucl. Phys. **A703** (2002) 489 [arXiv:hep-ph/0109115]; H. Weigert, Nucl. Phys. **A703** (2002) 823 [arXiv:hep-ph/0004044].
 - [13] D. Kharzeev, E. Levin and M. Nardi, Nucl. Phys. **A730** 448 (2004) [Erratum-ibid. **A743** 329 (2004)] [arXiv:hep-ph/0212316]; Phys. Rev. **C71** 054903 (2005) [arXiv:hep-ph/0111315]; D. Kharzeev and E. Levin, Phys. Lett. **B523** (2001) 79 [arXiv:nucl-th/0108006]; D. Kharzeev and M. Nardi, Phys. Lett. **B507** (2001) 121 [arXiv:nucl-th/0012025].
 - [14] D. Kharzeev, E. Levin and M. Nardi, Nucl. Phys. **A747** (2005) 609 [arXiv:hep-ph/0408050].
 - [15] Y. V. Kovchegov and K. Tuchin, Phys. Rev. **D65** (2002) 074026 [arXiv:hep-ph/0111362].
 - [16] M. A. Braun, Eur. Phys. J. **C48** (2006) 501 [arXiv:hep-ph/0603060]; Phys. Lett. **B483** (2000) 105.
 - [17] C. Marquet, Nucl. Phys. **B705** (2005) 319 [arXiv:hep-ph/0409023].
 - [18] A. Kovner and M. Lublinsky, JHEP **0611** (2006) 083 [arXiv:hep-ph/0609227].
 - [19] E. Levin and A. Prygarin, Phys. Rev. **C78** (2008) 065202 [arXiv:0804.4747 [hep-ph]].
 - [20] A. Kormilitzin, E. Levin and A. Prygarin, Nucl. Phys. **A813** (2008) 1 [arXiv:0807.3413 [hep-ph]].
 - [21] J. Bartels, M. Salvadore and G. P. Vacca, JHEP **0806** (2008) 032 [arXiv:0802.2702 [hep-ph]].
 - [22] K. Golec-Biernat and A. M. Stasto, Nucl. Phys. **B668** (2003) 345.
 - [23] E. Iancu, K. Itakura and S. Munier, Phys. Lett. **B590** (2004) 199 [arXiv:hep-ph/0310338].
 - [24] J. Bartels and E. Levin, Nucl. Phys. **B387** (1992) 617; A. M. Stasto, K. J. Golec-Biernat and J. Kwiecinski, Phys. Rev. Lett. **86** (2001) 596 [arXiv:hep-ph/0007192]; E. Iancu, K. Itakura and L. McLerran, Nucl. Phys. **A708** (2002) 327 [arXiv:hep-ph/0203137].
 - [25] E. Levin and K. Tuchin, Nucl. Phys. **B573** (2000) 833 [arXiv:hep-ph/9908317].
 - [26] G. Watt and H. Kowalski, Phys. Rev. **D78** (2008) 014016 [arXiv:0712.2670].

- [27] H. Kowalski, L. Motyka and G. Watt, Phys. Rev. **D74** (2006) 074016 [arXiv:hep-ph/0606272].
- [28] D. N. Triantafyllopoulos, Nucl. Phys. **B648** (2003) 293 [arXiv:hep-ph/0209121].
- [29] V. A. Khoze, A. D. Martin, M. G. Ryskin and W. J. Stirling, Phys. Rev. **D70** (2004) 074013 [arXiv:hep-ph/0406135].
- [30] J. L. Albacete and Y. V. Kovchegov, Phys. Rev. **D75** (2007) 125021 [arXiv:0704.0612].
- [31] S. J. Brodsky and G. R. Farrar, Phys. Rev. Lett. **31** (1973) 1153; V. A. Matveev, R. M. Muradian and A. N. Tavkhelidze, Lett. Nuovo Cim. **7** (1973) 719.
- [32] Y. L. Dokshitzer, V. A. Khoze and S. I. Troian, J. Phys. **G17** (1991) 1585.
- [33] V. A. Khoze, W. Ochs and J. Wosiek, arXiv:hep-ph/0009298; V. A. Khoze and W. Ochs, Int. J. Mod. Phys. **A12** (1997) 2949 [arXiv:hep-ph/9701421] and reference therein.
- [34] E. Gotsman, E. Levin, U. Maor and J. S. Miller, Eur. Phys. J. **C57** (2008) 689 [arXiv:0805.2799].
- [35] M. G. Ryskin, A. D. Martin and V. A. Khoze, Eur. Phys. J. **C54** (2008) 199 [arXiv:0710.2494].
- [36] A. A. Affolder *et al.* [CDF Collaboration], Phys. Rev. Lett. **87** (2001) 141802 [arXiv:hep-ex/0107070].
- [37] F. Abe *et al.* [CDF Collaboration], Phys. Rev. **D50** (1994) 5535.
- [38] K. Goulianos and J. Montanha, Phys. Rev. **D59** (1999) 114017 [arXiv:hep-ph/9805496].
- [39] F. Abe *et al.* [CDF Collaboration], Phys. Rev. **D50** (1994) 5550.
- [40] Y. L. Dokshitzer, hep-ph/9812252; hep-ph/0106348; G .P. Salam and D. Wicke, JHEP **0105** (2001) 061.
- [41] S. Eidelman *et al.* [Particle Data Group Collaboration], “*Review of particle physics*”, Phys. Lett. **B592** 1 (2004).
- [42] UA1 collaboration, Nucl. Phys. **B335** 261 (1990).
- [43] UA5 collaboration, Z. Phys. **C33** (1986) 1.
- [44] CDF collaboration, Phys. Rev. **D41** (1990) 2330; Phys. Rev. Lett. **61** (1988) 1819.
- [45] A. M. Rossi *et al.*, Nucl. Phys. **B84** (1975) 269.
- [46] B. Z. Kopeliovich, E. Levin, A. H. Rezaeian and I. Schmidt, Phys. Lett. **B675** (2009) 190; A. H. Rezaeian and A. Schaefer, arXiv:0908.3695.
- [47] S. Albino, B. A. Kniehl and G. Kramer, Nucl. Phys. **B803** (2008) 42.